A New Single-Logarithmic Approximation of Carson's Ground-Return Impedances–Part 1

INSU KIM, (Member, IEEE)
Department of Electrical Engineering, Inha University, Incheon 22212, South Korea

e-mail: insu@inha.ac.kr

ABSTRACT Distributed energy resources with unbalanced phases increase the power imbalance in a grid, and compensating for the imbalance requires accurate knowledge of the impedance of the transmission and distribution lines. To achieve such compensation, many studies have evaluated the series impedance of the lines. The previous studies can be classified into three categories: (a) studies that solved Carson's original equations (COEs), (b) those that approximated these equations by ignoring high-order terms, and (c) those that provided a closed-form solution for the equations. Solving the COEs requires the expansion of the improper integrals and infinite series. Therefore, the last approach is preferable for easier calculations and a small error. Thus, the objective of this study is to present a more accurate and robust closed-form solution. Toward this end, this study improves the single-logarithmic-approximation method by adding a fourth compensation term. That is, this study proposes the correction term $(2x/(x + \sqrt{1 + x^2}) \approx 1 - e^{-2x} - (x^3 e^{-2x})/3 + (x^5 e^{-5x})/5)$. This study substitutes the correction term to the original derivatives and finds their correct integrations to improve a single-logarithmic-approximation solution. The proposed solution was verified through case studies, and it showed fewer errors than the previous solutions. Additionally, the proposed solution can be also used to estimate the expected value of the self- and mutual impedance of overhead lines via stochastic simulations (e.g., Monte Carlo simulations), which will be presented in the second paper of this study.

INDEX TERMS Carson's equations, closed-form solution, mutual impedance, self-impedance.

NOMENCLATURE
ABBREVIATIONS
COE =	Carson's original equation
CRT =	common ratio term
CDER =	complex depth of earth return
DLA =	double-logarithmic closed-form approach
HOT =	high-order term
IS =	infinite series
SLA =	single-logarithmic closed-form approach

I. INTRODUCTION
Electrical loads are usually connected to power sources through transformers, transmission lines, distribution lines, or other power system equipment (e.g., capacitor banks, Var

compensators, voltage regulators, switches, circuit breakers, and protection relays). As the energy supplied by distributed energy sources increases, it can lead to an increase in the electric power imbalance. To compensate for the imbalance, we should accurately know the impedance of the lines.

Pollaczek and Carson derived the earth-return circuit impedance (i.e., the self- and mutual impedances of overhead lines parallel to the ground) [1], [2]. The self- and mutual impedances were defined by an improper integral, and Carson derived an infinite series (IS) expansion of the improper integral, which is referred to as Carson's original equations (COEs). It was not feasible to calculate the IS sum, therefore, many studies have obtained approximate solutions. For example, numerical IS approximation solutions have been found by using the Wedepohl-Wilcox IS formulation [3]. However, the study did not take the frequency-dependent ground condition into account, so closed-form approximation solutions were presented in various ground conditions that include

displacement currents [4]. The frequency characteristics of overhead transmission lines, dependent on the soil parameters, were also analyzed by adopting frequency-dependent soil models [5]. Since the previous models did not present a time-domain model, the time responses were assessed by injecting an impulse voltage to one of the wires when the terminal is opened [6]. Recently, an electromagnetic reciprocity method approximates the ground impedance correction parameters [7] and a conductor subdivision method calculates the ground impedance of buried cables [8]. These previous studies have tried to find the earth-return impedance, originally tackled by Pollaczek and Carson.

Meanwhile, the approximation approach, which presents a closed-form solution or ignores the higher-order terms (HOTs) of the IS, inherently includes errors. For example, the relative errors between approximation and algorithmic models were compared by contour images [9]. The third and more HOTs of the IS are sufficiently small to be ignored, so the second HOT of the IS (e.g., cos 2θ and sin 2θ terms) was defined as the knee point. The effect of the ignored HOTs on the accuracy was examined [10]. To reduce the error, the inverse Laplace transform of the improper integral form derived by Sunde provides an estimate of the transient ground resistance matrix [11], [12]. These recent approximation solutions show relatively good accuracy. For example, recently, a numerical algorithm was proposed to obtain a solution with nine significant digits for the COE [13]; the study also compared the solution with solutions derived from the models presented in [14]–[17]. An analytical solution with seven significant digits is also presented by using the exponential approximation of the COE [18]. However, these previous studies still show a difficulty in applying to stochastic Monte Carlo simulations that estimate the expected value of the self- and mutual impedances of overhead lines because the stochastic simulation requires a very large total number of calculations.

In the closed-form approach, the first-order Struve function and the second-kind first-order Bessel function represent solutions of the COE [19]. One method to find a closed-form solution to the COE is to replace the earth under overhead lines by the image conductors of the lines; this is known as the image method [20]–[22]. In another approach, the image conductors are assumed to have a complex depth of earth return (CDER) and their impedance is assumed to be influenced by the soil skin depth [16], and the obtained solution has also been mathematically proved to be a single-logarithmic closed-form approach (SLA) solution [15]. In particular, the approximation $2x/(x + \sqrt{1 + x^2}) \approx 1 - e^{-2x}$ is used for obtaining the SLA solution [15]. One study, [14], added the correction term $(2x/(x + \sqrt{1 + x^2}) \approx 1 - e^{-2x} - (x^3 e^{-2x})/3)$ to the CDER model to reduce errors, and thereby improved the accuracy of the SLA solution of [15].

The double-logarithmic closed-form approach (DLA) has been proposed for obtaining more accurate solutions. For example, the coefficients $A = 0.1159$, $B = 0.8841$,

$\alpha = 0.2258$, and $\beta = 1.1015$ have been used for obtaining the DLA solution [23]. The previous DLA of [23] was improved by optimizing the coefficients [17]. Based on a combination of Chebyshev expansions and rational approximations, an algorithm for computing the Struve and Bessel functions in the COEs has been presented for MATLAB [24].

The previous studies have approximated the self- and mutual impedances of transmission and distribution lines by either ignoring HOTs or providing closed-form solutions. However, none of the previous studies improved the SLA modified in [14]. The present study derives an improved SLA solution. For obtaining the solution, this study enhances the previous SLA in [14] by adding a fourth compensation term. That is, this study adds a fourth compensation term using $(2x/(x + \sqrt{1 + x^2}) \approx 1 - e^{-2x} - (x^3 e^{-2x})/3 + (x^5 e^{-5x})/5)$. The proposed SLA is compared with previous approaches (e.g., COE, CDER, double logarithmic, and Struve function evaluation models) for a broad range of frequencies and ground resistivities, to provide the robustness of the proposed method. Through case studies of transmission and distribution lines, it is shown that the proposed additional compensation term reduces errors in the solution of the COEs, at the cost of slightly increasing the calculation time compared to that of the previous SLA in [14]. For example, the proposed method increases the calculation speed (e.g., 14.20%, 16.13%, or 16.69 %), compared to the previous SLA method in the three case studies. However, the proposed method improves the average accuracy of 11.49% for a distribution line example, compared to that of the previous SLA. As a result, the proposed method with fewer errors will be applied to stochastic Monte Carlo simulations that evaluate the expected value of the self- and mutual impedances of overhead lines. The detailed methods and results of finding the expected value will be presented in the second paper of this study.

The rest of this paper is organized as follows. Section 2 briefly introduces the general form of the COEs and previously proposed SLAs and DLAs. In Section 3, the proposed SLA solution is derived, and Section 4 presents case studies that validate the accuracy of the proposed SLA. Finally, Section 5 summarizes the conclusions of this study.

II. CARSON'S GROUND RETURN CIRCUIT IMPEDANCE
A. CARSON'S ORIGINAL EQUATIONS
Fig. 1 shows two current-carrying conductors i and j and their earth-return images (i' and j'). Carson and Pollaczek separately derived the improper integral for the ground return impedance [1], [2] and Sunde reformulated it [22].

$$Z = \frac{j\omega\mu_0}{2\pi} \ln\left(\frac{D_2}{D_1}\right)$$
$$+ \frac{j\omega\mu}{\pi} \int_0^\infty \left(\frac{e^{-H\lambda}}{\lambda + \sqrt{\lambda^2 + j\omega\mu\sigma}}\right) \cos(x\lambda) d\lambda, \quad (1)$$
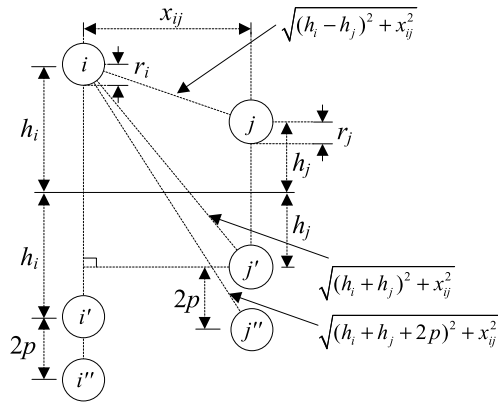
FIGURE 1. Two conductors with their earth-return conductors [1].

where

$\omega =$	angular frequency (rad/s);
μ_0 and $\mu =$	permeabilities of free space and the ground, respectively;
$\sigma =$	conductivity of the ground.

For the self-impedance, $D_1 = r_i$ (radius of the conductor i), $D_2 = 2h_i$ (height of the conductor i), $H = D_2$, and $x = 0$. For the mutual impedance, $D_1 = \sqrt{(h_i - h_j)^2 + x_{ij}^2}$, $D_2 = \sqrt{(h_i + h_j)^2 + x_{ij}^2}$, $H = h_i + h_j$, and $x = x_{ij}$.

B. EXISTING APPROXIMATION MODELS

COEs used for calculating self and mutual series impedances require an improper integral. In closed-form approximation approaches, a long calculation time may be required for calculating the IS (to solve the improper integral) for a broad range of frequencies. For example, in [1] and [25], the self-impedance (Z_s) and mutual impedance (Z_m) for $\mu = \mu_0$ were approximated as

$$Z_s = \frac{j\omega\mu_0}{2\pi} \ln \frac{2h_i}{r_i} + \frac{j\omega\mu}{\pi} J_s, \tag{2}$$

$$Z_m = \frac{j\omega\mu_0}{2\pi} \ln \frac{\sqrt{(h_i + h_j)^2 + x_{ij}^2}}{\sqrt{(h_i - h_j)^2 + x_{ij}^2}} + \frac{j\omega\mu}{\pi} J_m, \tag{3}$$

$$J_s = \int_0^\infty \left(\frac{e^{-2h_i\lambda}}{\lambda + \sqrt{\lambda^2 + j\omega\mu\sigma}} \right) d\lambda \approx \frac{1}{2} \ln \left(\frac{p}{h_i} + 1 \right), \tag{4}$$

$$J_m = \int_0^\infty \left(\frac{e^{-(h_i + h_j)\lambda}}{\lambda + \sqrt{\lambda^2 + j\omega\mu\sigma}} \right) \cos(x_{ij}\lambda) d\lambda$$
$$\approx \frac{1}{2} \ln \frac{\sqrt{(h_i + h_j + 2p)^2 + x_{ij}^2}}{\sqrt{(h_i + h_j)^2 + x_{ij}^2}}, \tag{5}$$

where

$$p = \sqrt{\frac{1}{j\omega\mu\sigma}}.$$

The self- and mutual impedance were then simplified by adding $2p$:

$$Z_s \approx \frac{j\omega\mu_0}{2\pi} \ln \frac{(2h_i + 2p)}{r_i}, \tag{6}$$

$$Z_m \approx \frac{j\omega\mu_0}{2\pi} \ln \frac{\sqrt{(h_i + h_j + 2p)^2 + x_{ij}^2}}{\sqrt{(h_i - h_j)^2 + x_{ij}^2}}. \tag{7}$$

In Fig. 1, the addition of $2p$, which is referred to as the CDER term, corresponds to the replacement of the image conductors i' and j' with i'' and j'', respectively. Indeed, the CDER model is an example of an SLA. The SLA was enhanced in [14] by using the approximation

$$\frac{2\lambda}{\lambda + \sqrt{\lambda^2 + 1}} \approx 1 - e^{-2\lambda} - \frac{1}{3}\lambda^3 e^{-2\lambda}. \tag{8}$$

A DLA was proposed in [23] and another DLA was improved in [17]. The study in [17] expressed the improper integral term by using the first-order $\mathbf{H}_1(u)$ of the Struve function and the second-kind first-order Bessel function $Y_1(u)$:

$$\int_0^\infty \left(\frac{2e^{-H\lambda}}{\lambda + \sqrt{\lambda^2 + j\omega\sigma}} \right) \cos(x\lambda) d\lambda$$
$$= \frac{\pi}{2u_1} [\mathbf{H}_1(u_1) - Y_1(u_1)] - \frac{1}{u_1^2}$$
$$+ \frac{\pi}{2u_2} [\mathbf{H}_1(u_2) - Y_1(u_2)] - \frac{1}{u_2^2}, \tag{9}$$

where $u_1 = \sqrt{j\omega\mu\sigma}(H - jx)$ and $u_2 = \sqrt{j\omega\mu\sigma}(H + jx)$. The detailed definitions of $\mathbf{H}_1(u)$ and $Y_1(u)$ are presented in [19].

An analytical solution of the COE was presented by computing $\mathbf{H}_1(z)$ and $Y_1(z)$ separately for a range of $|z| \le z_0$ and $\mathbf{H}_1(z) - Y_1(z)$ for $|z| \ge z_0$ [24].

III. PROPOSED COMPENSATED SINGLE LOGARITHMIC APPROACH

The objective of this study was to improve the SLA presented in [14]. Toward this end, for the example in Fig. 1 the following variables were initially defined.

$$w = p\lambda, \tag{10}$$
$$\beta = x/(h_i + h_j), \tag{11}$$
$$q_1 = \frac{h_i}{p}, \tag{12}$$
$$q_2 = (h_i + h_j)/2p. \tag{13}$$

The substitution of (10)-(13) into (4) and (5) yields

$$J_s(q_1) = \int_L \left(\frac{e^{-2q_1 w}}{w + \sqrt{w^2 + 1}} \right) dw, \tag{14}$$

$$J_m(q_2) = \frac{1}{2} \int_L \left(\frac{e^{-2(1+j\beta)q_2 w} + e^{-2(1-j\beta)q_2 w}}{w + \sqrt{w^2 + 1}} \right) dw. \tag{15}$$

The derivatives of (14) and (15) with respect to q_1 and q_2 are

$$\frac{dJ_s(q_1)}{dq_1} = -\int_0^\infty \left(\frac{2w}{w + \sqrt{w^2 + 1}} \right) e^{-2q_1 w} dw. \tag{16}$$

$$\frac{dJ_m(q_2)}{dq_2} = -\frac{1}{2}\int_0^\infty \left(\frac{2w}{w+\sqrt{w^2+1}}\right)$$
$$\times \left((1+j\beta)e^{-2(1+j\beta)q_2 w}\right.$$
$$\left. + (1-j\beta)e^{-2(1-j\beta)q_2 w}\right) dw. \tag{17}$$

The proposed method approximates the first term in (16) and (17) as

$$\frac{2w}{w+\sqrt{w^2+1}} \approx 1 - e^{-2w} - \frac{1}{3}w^3 e^{-2w} + \frac{1}{5}w^5 e^{-5w}. \tag{18}$$

Substituting (18) in (16) and (17) gives

$$\frac{dJ_s(q_1)}{dq_1} \approx -\int_0^\infty \left(1 - e^{-2w} - \frac{1}{3}w^3 e^{-2w} + \frac{1}{5}w^5 e^{-5w}\right)$$
$$\times e^{-2q_1 w} dw, \tag{19}$$

$$\frac{dJ_m(q_2)}{dq_2} \approx -\frac{1}{2}\int_0^\infty \left(1 - e^{-2w} - \frac{1}{3}w^3 e^{-2w} + \frac{1}{5}w^5 e^{-5w}\right)$$
$$\times \left((1+j\beta)e^{-2(1+j\beta)q_2 w}\right.$$
$$\left. + (1-j\beta)e^{-2(1-j\beta)q_2 w}\right) dw. \tag{20}$$

The integration of (19) yields

$$J_s(q_1) \approx -\frac{1}{2}\ln(q_1) + \frac{1}{2}\ln(q_1 + 1)$$
$$- \frac{1}{24}(q_1 + 1)^{-3} + \frac{12}{5}(2q_1 + 5)^{-5}, \tag{21}$$

and the integration of (20) gives

$$J_m(q_2) \approx -\frac{1}{2}\ln(q_2) + \frac{1}{4}\ln\left(q_2 + \frac{1}{1+j\beta}\right)$$
$$+ \frac{1}{4}\ln\left(q_2 - \frac{1}{-1+j\beta}\right) + J_1 + J_2, \tag{22}$$

where, (23) as shown at the bottom of the page.

The derivation of J_1 and J_2 is one of the contributions of this paper.

IV. CASE STUDIES
A. ACCURACY VALIDATION OF THE PROPOSED METHOD
This study compared the series impedance determined by the proposed model with those determined in [14]–[16], [24], [26]–[28]. As a reference, this study solved the COE containing the nth HOT of the IS derived from the improper integral [26]. The reference solution is denoted by $\mathbf{Z}_{\text{ref}}$. The CDER model from [15], [16] and the compensated SLA model from [14] were implemented in MATLAB, and

TABLE 1. Practical ranges of parameters.

Parameter	Range
Frequency f [26]	10^{-1} Hz to 10^5 Hz
Ground resistivity ρ $(=1/\sigma)$ [17]	1 Ω·m to 10 kΩ·m
Vertical distance of conductors (i.e., h) [17]	5 mm to 200 m
Horizontal distance of conductors (i.e., x) [28, 29]	1.0–20.0 m

they are denoted by $\mathbf{Z}_{\text{CDER}}$ and $\mathbf{Z}_{\text{SLA}}$, respectively. Furthermore, the simplified model of [27], [28] was implemented in MATLAB, and it is denoted by $\mathbf{Z}_{\text{sim}}$. The recent analytical calculation model of [24] was also implemented, and it is denoted by $\mathbf{Z}_{\text{Theo}}$. To verify the proposed method, this study calculated the impedance matrix for the practical ranges of parameters, which are presented in TABLE 1.

1) SOLVING THE FULL COEs
To determine the reference self- and mutual impedance ($\mathbf{Z}_{\text{ref}}$), this study solved the full COEs for the simple two-conductor system shown in Fig. 2. The system includes two 336,400 26/7 ACSR Linnet cables. Subsequently, the effect of the highest-order term to be retained in the IS in the COEs on the convergence of the solution (i.e., self- and mutual impedance) was examined.
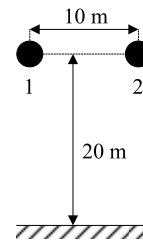
FIGURE 2. Simple two-conductor system.

The frequency and ground resistivity ranges were defined as $[f_{\text{min}}, f_{\text{max}}] = [0.1 \text{ Hz}, 10^5 \text{ Hz}]$ and $[\rho_{\text{min}}, \rho_{\text{max}}] = [1 \Omega \cdot \text{m}, 10 \text{ k}\Omega \cdot \text{m}]$ on the basis of TABLE 1. The common ratio term (CRT) (e.g., the $[r]$ term in [1] or the $[a]$ term in [26]), which is proportional to the square root of the frequency and inversely proportional to the square root of the ground resistivity, is defined in the COEs. Since the HOTs are multiplied by the power order of the CRT (e.g., the nth term is multiplied by r^n), the IS converges rapidly for a CRT (i.e., r) ≤ 2 [1]. For a CRT (i.e., r) > 5, the IS is approximated by a finite series, or calculations are performed up to the seventh HOT [26], [30]. For example, this study identified the case that converged the slowest at the frequency and ground

$$J_1 = \frac{-(q_2 + 1)\left(-3\beta^2 q_2^2 + q_2^2 + 2q_2 + 1\right)}{24\left(\beta^2 q_2^2 + q_2^2 + 2q_2 + 1\right)^3},$$

$$J_2 = \frac{12(2q_2 + 5)\left(80\beta^4 q_2^4 - 160\beta^2 q_2^4 - 800\beta^2 q_2^3 - 1000\beta^2 q_2^2 + 16q_2^4 + 160q_2^3 + 600q_2^2 + 1000q_2 + 625\right)}{5\left(4\beta^2 q_2^2 + 4q_2^2 + 20q_2 + 25\right)^5} \tag{23}$$
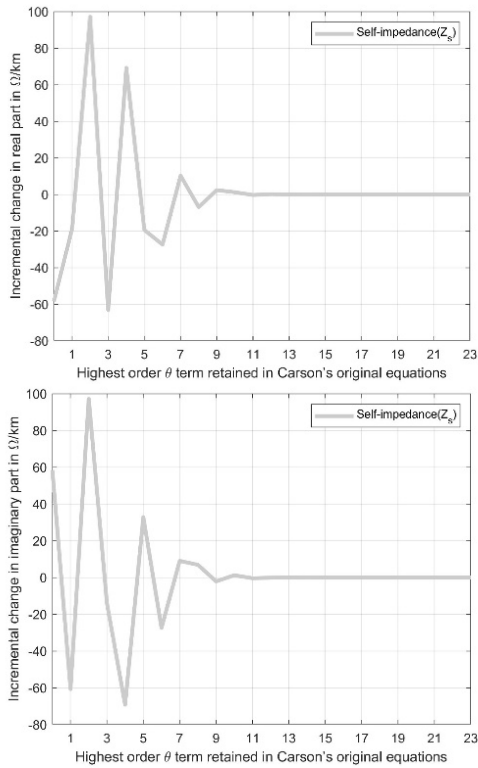
FIGURE 3. Incremental change in the self-impedance when the order of the highest-order term was increased.

(a) self-impedance

(b) mutual impedance

FIGURE 4. Convergence of the self- and mutual impedance.

resistivity intervals considered. The CRT was 4.9945 at a frequency of 19.745 kHz and a ground resistivity of $10\,\Omega \cdot$ m. Fig. 3 presents the incremental change in the self-impedance in ohms per kilometer for the case $r = 4.9945$ when the order of the highest-order term increased. When terms up to the 24th order term of the IS were retained, the incremental change in the self-impedance relative to the self-impedance when terms up to the 23rd order were retained was almost zero (e.g., at the sixth decimal place).

Fig. 4 shows the convergence curve of the self-impedance. In Fig. 4 (a) and (b), the self-impedance converges to the solution ($5.524254 + j219.9318\ \Omega$/km) and the mutual impedance converges to $5.16361 + j41.5803\ \Omega$/km. The 25th and HOTs are negligible, or zero up to the sixth decimal place. Thus, this study calculated the nth HOT of the IS and used the criterion that the incremental change is less than 10^{-6} as the reference ($\mathbf{Z}_{\text{ref}}$) to verify the accuracy of the proposed method.

2) FOUR-WIRE OVERHEAD LINE

For the verification of the accuracy of the proposed method, the four-wire overhead distribution line in Fig. 5 was modeled [28]. The system included phase conductors (336,400 26/7 ACSR Linnet) and a neutral conductor (4/0 6/1 ACSR). Detailed data of these conductors are available in Appendix A in [28].

At a frequency of 60 Hz and a ground resistivity of $100\ \Omega \cdot$m, the 3×3 impedance matrix (in ohms per kilometer)
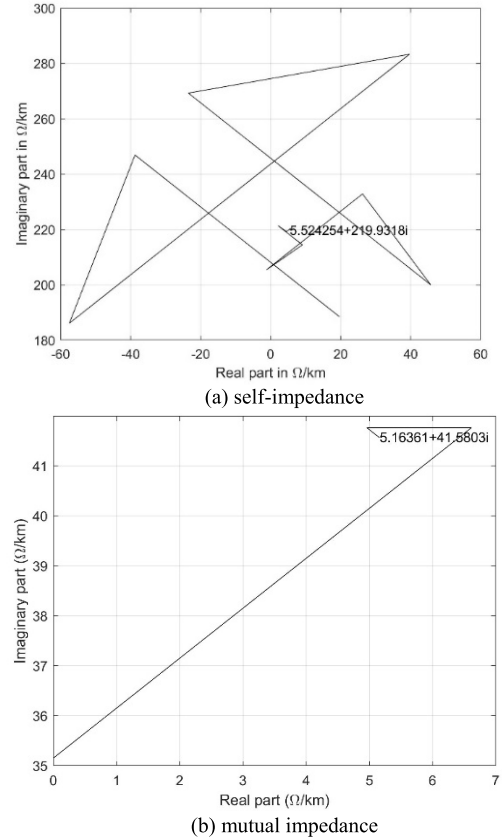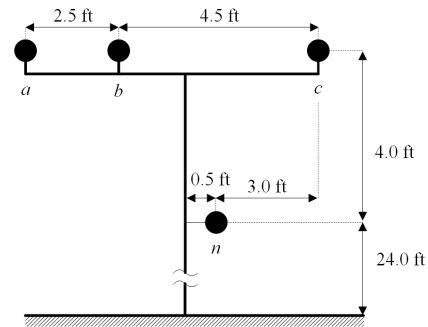

FIGURE 5. Four-wire overhead line [28].

of the reference model is Eq. (24), as shown at the bottom of the next page.

The CDER model (as an example of an SLA) yields the impedance matrix Eq. (25), as shown at the bottom of the next page.

The average percent difference between the absolute value of this 3×3 impedance matrix and that of (24) is 0.50119%. The SLA model improved by [14] gives the impedance matrix Eq. (26), as shown at the bottom of the next page.

The average percent difference between the absolute value of this impedance matrix and that of (24) is 0.00539%, which is better than the accuracy of (25). The proposed model

($\mathbf{Z}_{\text{proposed}}$) yields the impedance matrix Eq. (27), as shown at the bottom of the page.

The proposed method shows the lowest average percent difference, 0.005%, from the absolute value of (24). $\mathbf{Z}_{\text{sim}}$ and $\mathbf{Z}_{\text{Theo}}$ showed average percent differences of 0.14131% and 3.86687%, respectively.

The average percent difference for the 3 × 3 impedance matrix when the frequency was varied from 0.1 Hz to 100 kHz at a fixed ground resistivity of 100 Ω · m is plotted in Fig. 6. For the real part, the proposed method showed the smallest difference from the reference in the full frequency range, except the range 15–40 Hz, and around 5 kHz, and the simplified model ($\mathbf{Z}_{\text{sim}}$) showed the largest difference from the reference at the frequency of 200 Hz or above. For the imaginary part, the proposed method showed a larger difference than the compensated SLA model ($\mathbf{Z}_{\text{SLA}}$) in the ranges 40–1 kHz and 25–100 kHz, and the CDER model ($\mathbf{Z}_{\text{CDER}}$) showed a larger difference than the proposed method at the full frequency. For both the real and imaginary parts, the analytical calculation model ($\mathbf{Z}_{\text{Theo}}$) showed a larger difference than the proposed method in the full frequency range, except at the frequency of 2 Hz and below. For the absolute value of the 3 × 3 impedance matrix, the $\mathbf{Z}_{\text{Theo}}$, $\mathbf{Z}_{\text{CDER}}$, and $\mathbf{Z}_{\text{sim}}$ models showed a larger difference than the $\mathbf{Z}_{\text{proposed}}$ and $\mathbf{Z}_{\text{SLA}}$ models, except at the frequency of 3 Hz or below. By contrast, for the absolute value, the proposed method showed a smaller difference than the compensated SLA ($\mathbf{Z}_{\text{SLA}}$) model in the full frequency range, except in the ranges 70–1 kHz and 25–100 kHz.

Fig. 7 shows the average percent differences between different models to the reference model when the ground resistivity was varied from 1 Ω·m to 10 kΩ·m at a fixed frequency of 60 Hz.

For the real part, the proposed method showed the least difference from the reference in the range 1–300 Ω · m.
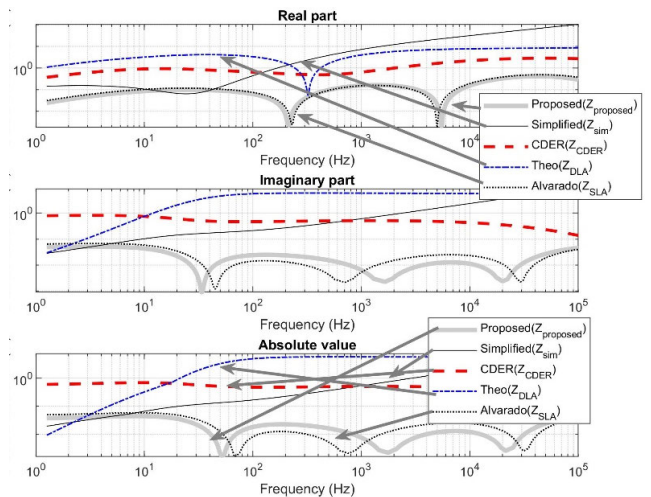

FIGURE 6. Comparison of the average percent difference for real and imaginary parts and absolute values (in the frequency range of 0.1 to 10 MHz).

In fact, the proposed method shows a smaller difference than the compensated SLA model in all frequency ranges. However, the simplified model exhibited a smaller difference than the proposed method at the ground resistivity of 300 Ω · m and above. For the imaginary part, the proposed method showed the least difference from the reference in the range 1–30 Ω · m. The compensated SLA model ($\mathbf{Z}_{\text{SLA}}$) showed the least difference in the range from 30 Ω · m to 2.5 kΩ · m, while the simplified model exhibited the least difference in the range 2.5–10 kΩ · m. For the absolute value of the 3 × 3 impedance matrix, the proposed method showed the least difference at ground resistivities of 100 Ω · m and below.

Next, this study determined the effect of the HOTs in the ground resistivity interval $[\rho_{\min}, \rho_{\max}] = [1\,\Omega\cdot\text{m}, 10\,\text{k}\Omega\cdot\text{m}]$

$$\mathbf{Z}_{\text{ref}} = \begin{bmatrix} 0.28407+0.67051i & 0.096677+0.31235i & 0.095135+0.23982i \\ 0.096677+0.31235i & 0.28974+0.65192i & 0.097962+0.26387i \\ 0.095135+0.23982i & 0.097962+0.26387i & 0.28652+0.66243i \end{bmatrix}. \tag{24}$$

$$\mathbf{Z}_{\text{CDER}} = \begin{bmatrix} 0.28498+0.67214i & 0.097597+0.31392i & 0.09605+0.24143i \\ 0.097597+0.31392i & 0.29067+0.65343i & 0.098885+0.26541i \\ 0.09605+0.24143i & 0.098885+0.26541i & 0.28744+0.66401i \end{bmatrix}. \tag{25}$$

$$\mathbf{Z}_{\text{SLA}} = \begin{bmatrix} 0.28395+0.67052i & 0.096553+0.31238i & 0.095013+0.23984i \\ 0.096553+0.31238i & 0.28961+0.65196i & 0.097836+0.2639i \\ 0.095013+0.23984i & 0.097836+0.2639i & 0.28639+0.66246i \end{bmatrix}. \tag{26}$$

$$\mathbf{Z}_{\text{proposed}} = \begin{bmatrix} 0.28396+0.67056i & 0.096571+0.31241i & 0.095031+0.23988i \\ 0.096571+0.31241i & 0.28963+0.65199i & 0.097854+0.26393i \\ 0.095031+0.23988i & 0.097854+0.26393i & 0.28641+0.66249i \end{bmatrix}. \tag{27}$$
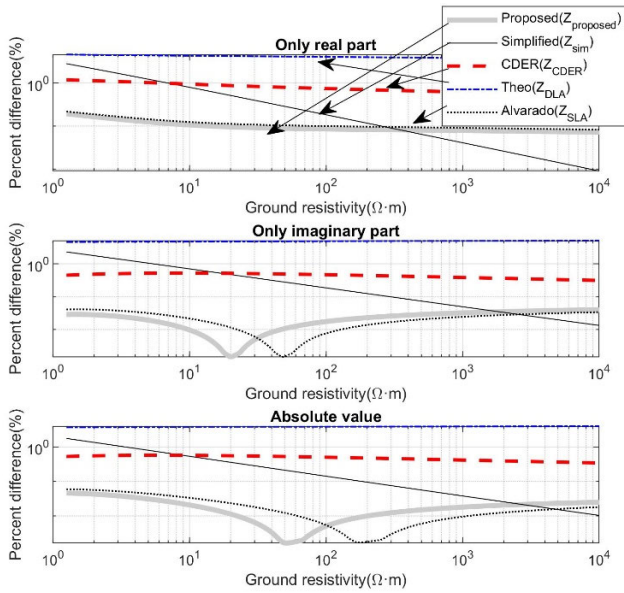
FIGURE 7. Comparison of the average percent difference for the real and imaginary parts and for absolute values (in the resistivity range 1–10 kΩ · m.
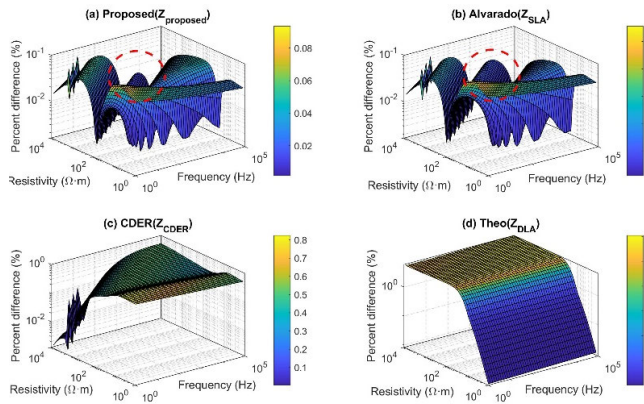

FIGURE 8. Comparison of the average percent difference for the absolute value.

and the frequency interval $[f_{\min}, f_{\max}] = [0.1 \text{ Hz}, 100 \text{ kHz}]$. Fig. 8 shows percent differences for the absolute value of the 3×3 impedance matrix. The proposed and compensated models $\mathbf{Z}_{\text{proposed}}$ and $\mathbf{Z}_{\text{SLA}}$ in Fig. 8 (a) and (b) show similar percent differences from the reference at the ground resistivity and frequency intervals considered, because of the similar approximations derived in (8) and (18). They also show a smaller difference from the reference than the $\mathbf{Z}_{\text{CDER}}$ and $\mathbf{Z}_{\text{Theo}}$ models, in Fig. 8 (c) and (d). However, the detailed comparison between both the models indicates the proposed method with fewer percent relative differences to the $\mathbf{Z}_{\text{SLA}}$ model, particularly in the dashed circle area.

The difference between the proposed and previous models is evident in TABLE 2, which summarizes the average percent difference from the reference for the absolute values of the 3×3 impedance matrix in the ground resistivity and

TABLE 2. Summary of the average percent difference from the absolute value of the reference model.

Method	Minimum (%)	Maximum (%)	Average (%)
Proposed model ($\mathbf{Z}_{\text{proposed}}$)	0.001595	0.09358	0.02858
Compensated SLA ($\mathbf{Z}_{\text{SLA}}$)	0.001605	0.11157	0.03229
CDER ($\mathbf{Z}_{\text{CDER}}$)	0.001256	0.82488	0.46305
Analytical model ($\mathbf{Z}_{\text{Theo}}$)	0.008283	6.04696	3.95257
Simplified model ($\mathbf{Z}_{\text{sim}}$)	0.001714	40.34273	2.47008

frequency intervals considered. Clearly, in the table, the simplified model shows the largest average difference in the absolute value, which is because the model is usually used for a low frequency. The compensated SLA model improves the accuracy of the CDER model from 0.46305% to 0.03229%. The proposed model shows the least average percent difference, and it improves the accuracy of the compensated SLA model from 0.03229% to 0.02858% because of the fourth added term in (18), which means the improvement in the accuracy by as much as 11.49%.

Typical overhead transmission and distribution power lines deliver electrical power across long distances at a low frequency (e.g., 50 or 60 Hz). In addition to the low frequency, the geometrical location of the phase conductors in Fig. 2 and Fig. 5 is an example. Moreover, line sags and imbalances in phase conductors affect the relative percent difference. To the impact of line sages and imbalances in phase conductors on the accuracy improvement of the proposed method, the stochastic method (e.g., Monte Carlo simulation and finite element methods) will be presented in the second paper of this study.

3) EXAMPLE OF A TRANSMISSION LINE
The proposed model was applied to a 500 kV transmission line with a frequency of 50 Hz; the transmission line is shown in Fig. 9 [31]. The system includes 12 Panther (30/3+7/3 ACSR) bundled cables (with a conductor conductivity of 25785150 m/Ω, an earth resistivity of 100 Ω · m, a GMR of 1.049 cm, and an internal radius of 0.453 cm). The neutral wires were ignored. The detailed data are available in [31].

The 3×3 impedance matrix (in ohms per kilometer) of the reference model ($\mathbf{Z}_{\text{ref}}$) is Eq. (28), as shown at the bottom of the page.

The 3×3 impedance matrix of the CDER model is given by Eq. (29), as shown at the bottom of the page. which is the same matrix presented in [31]. Equation (29) includes average percent differences of 1.05641%, 1.32038%, and 1.31185% relative to the real and imaginary parts and absolute values of (28). The impedance matrix of the analytical model is Eq. (30), as shown at the bottom of the page.

The average percent differences relative to the real and imaginary parts and absolute values of (28) are 0.00072%, 0.54104%, and 0.52882%, respectively. The impedance
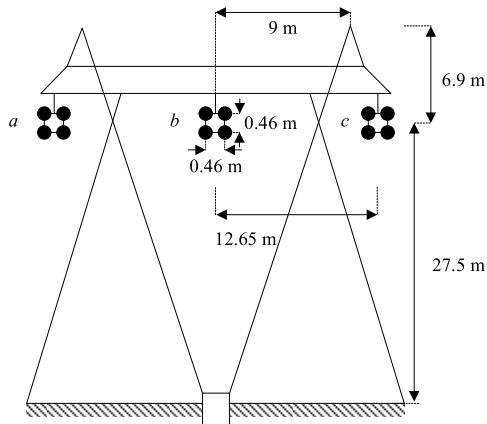
FIGURE 9. Example of a 500 kV transmission line [31].

TABLE 3. Average percent differences for the real and imaginary parts.

Method	Real part (%)	Imaginary part (%)
Proposed model ($\mathbf{Z}_{proposed}$)	0.44575	0.10814
Compensated SLA model ($\mathbf{Z}_{SLA}$)	0.46873	0.12997
CDER ($\mathbf{Z}_{CDER}$)	1.66971	0.94953
Analytical model ($\mathbf{Z}_{Theo}$)	0.25596	0.57796
Simplified model ($\mathbf{Z}_{sim}$)	44.36109	9.16242

simplification of the COE by the assumption that the model is usually used for a low power system frequency. In fact, the model results in a large error at high frequencies. For the real part, the analytical model showed the least average difference (0.25596% for $\mathbf{Z}_{Theo}$ vs. 0.44575% for $\mathbf{Z}_{proposed}$). By contrast, for the imaginary part, the proposed method showed the least average difference (0.10814% for $\mathbf{Z}_{proposed}$ vs. 0.57796% for $\mathbf{Z}_{Theo}$). The proposed method improves the accuracy of the compensated SLA model ($\mathbf{Z}_{SLA}$) by as much as 4.9% (for a real part) and 16.8% (for an imaginary part). Thus, the proposed method was closer than the other models, including the analytical model, to the reference.

matrix of the compensated SLA model is Eq. (31), as shown at the bottom of the page.
with the average percent differences for the real and imaginary parts and absolute values relative to (28) being 0.08566%, 0.16987%, and 0.16213%, respectively. The impedance matrix of the proposed model is Eq. (32), as shown at the bottom of the page.

The proposed model is superior to the aforementioned models, with reducing average percent differences of 0.09830%, 0.14123%, and 0.13398% for the real and imaginary parts and absolute values, respectively.

This study varied the frequency from 0.1 Hz to 100 kHz and the ground resistivity from $1\,\Omega\cdot m$ to $10\,k\Omega\cdot m$, as shown in TABLE 1. TABLE 3 compares the average percent differences for the real and imaginary parts for the different models relative to the reference model. Clearly, the compensated SLA model improved the accuracy of the CDER model. The simplified model showed the largest difference because of the

This study changed the horizontal position of a one-phase group (e.g., phase c conductors) in Fig. 9. The frequency was set as 50 Hz and the ground resistivity as $100\,\Omega\cdot m$. Fig. 10 presents the absolute value of the mutual impedance (i.e., Z_{ac}) when the horizontal distance of the phase c conductors from the middle of the system was increased. At the original horizontal distance of phase group c (e.g., 12.42 m and 12.88 m), the mutual impedance ($Z_{m,ac}$) was $0.046399 + 0.22979i\ \Omega/km$, which is identical to that in (28). As the horizontal distance (i.e., x_{ac}) increased, the D_1 and D_2 terms of the first part in (1) or (7) gradually became equal. Therefore, the magnitude of the mutual impedance in Fig. 10 decreased. To clarify the difference between each model and the reference, the average percent differences of the 3×3 impedance

$$\mathbf{Z}_{ref} = \begin{bmatrix} 0.080935+0.53547i & 0.046443+0.2733i & 0.046399+0.22979i \\ 0.046443+0.2733i & 0.080941+0.53546i & 0.046443+0.2733i \\ 0.046399+0.22979i & 0.046443+0.2733i & 0.080935+0.53547i \end{bmatrix} \tag{28}$$

$$Z_{CDER} = \begin{bmatrix} 0.081497+0.53958i & 0.047011+0.27741i & 0.046985+0.23388i \\ 0.047011+0.27741i & 0.081503+0.53957i & 0.047011+0.27741i \\ 0.046985+0.23388i & 0.047011+0.27741i & 0.081497+0.53958i \end{bmatrix}, \tag{29}$$

$$\mathbf{Z}_{Theo} = \begin{bmatrix} 0.080936+0.52684i & 0.046443+0.27328i & 0.046398+0.22978i \\ 0.046443+0.27328i & 0.080942+0.52683i & 0.046443+0.27328i \\ 0.046398+0.22978i & 0.046443+0.27328i & 0.080936+0.52684i \end{bmatrix}. \tag{30}$$

$$\mathbf{Z}_{SLA} = \begin{bmatrix} 0.080978+0.53495i & 0.046488+0.27278i & 0.04645+0.22925i \\ 0.046488+0.27278i & 0.080984+0.53493i & 0.046488+0.27278i \\ 0.04645+0.22925i & 0.046488+0.27278i & 0.080978+0.53495i \end{bmatrix}, \tag{31}$$
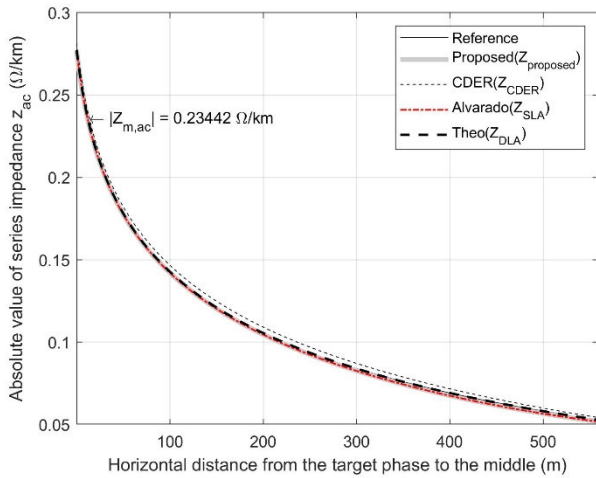
FIGURE 10. Mutual impedance (Z_{ac}) when the horizontal distance of conductor bundle group *c* from the middle of the system was increased.
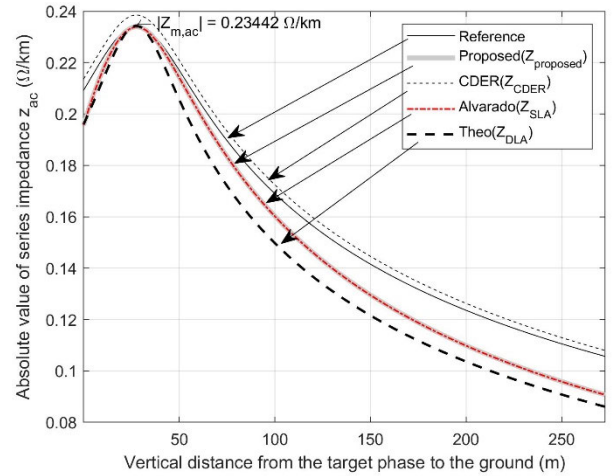

FIGURE 12. Mutual impedance (Z_{ac}) when the vertical distance of conductor bundle group *a* from the ground increased.
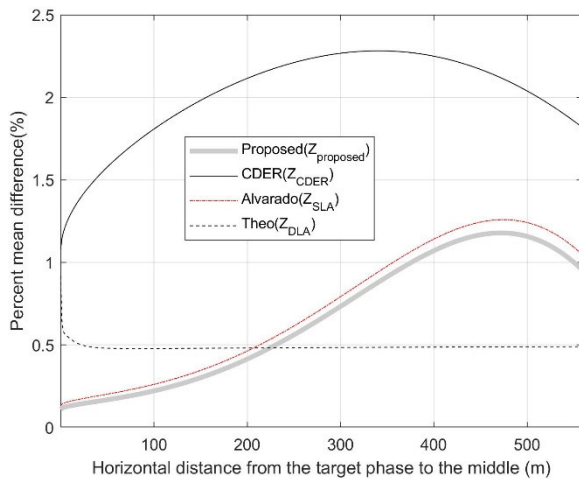

FIGURE 11. Average percent difference when the horizontal distance of phase *c* from the middle of the system increased.

matrix of each model relative to the reference model were determined, and they are presented in Fig. 11. The CDER model showed the highest difference at a high x/h ratio, which is comparable to that in [14]. For horizontal distances less than about 200 m, the proposed model showed the least difference. For the distance range 200–550 m, the analytical model showed the least difference. However, the proposed model showed better accuracy than the compensated SLA model at the full distance. Within the feasible range of the horizontal distance presented in TABLE 1, the proposed model was the most accurate.

The vertical distance of a one-phase bundle group (e.g., phase *a* conductors) was varied in this study. At the

original vertical distance of phase group *c* (e.g., 27.5 m and 27.96 m), the mutual impedance ($Z_{m,ac}$) was $0.046399 + 0.22979i$ Ω/km. Fig. 12 presents the absolute value of the mutual impedance (i.e., Z_{ac}). As the vertical distance of the phase *a* group increased, the D_1 and D_2 terms of the first part in (1) or (7) gradually became equal, resulting in a decrease in the mutual impedance, which is evident in Fig. 12. The CDER model showed the least difference relative to the reference. Both the $\mathbf{Z}_{proposed}$ and $\mathbf{Z}_{SLA}$ models showed almost identical accuracies. The analytical model ($\mathbf{Z}_{Theo}$) showed the largest difference.

Fig. 13 shows the average percent difference of the 3×3 impedance matrix of each model. Clearly, before the distance of about 75 m, the proposed method showed the least difference. However, after about 75 m, the CDER model showed the least difference. In the full range of the distance, the proposed method showed better accuracy than the compensated SLA model. The absolute value of the self-impedance (i.e., Z_{aa}) was examined when the vertical distance of the one-phase bundle group (e.g., the phase *a* conductors) was varied. Fig. 14 presents the absolute value of the self-impedance. At the original vertical distance of phase group *a* (e.g., 27.5 m and 27.96 m), the self-impedance (Z_{aa}) was $0.080935 + 0.53547i$ Ω/km, which is identical to that in (28). The analytical model ($\mathbf{Z}_{Theo}$) showed the largest difference for the full distance range. To examine the accuracy of each model relative to the reference, this study determined the average percent differences for the real and imaginary parts of the 3×3 impedance matrix for each model, and they are shown in Fig. 15. For the real part, the analytical model showed the least difference. However, for the imaginary part, the

$$\mathbf{Z}_{proposed} = \begin{bmatrix} 0.080985+0.53503i & 0.046495+0.27287i & 0.046457+0.22934i \\ 0.046495+0.27287i & 0.080991+0.53502i & 0.046495+0.27287i \\ 0.046457+0.22934i & 0.046495+0.27287i & 0.080985+0.53503i \end{bmatrix}. \tag{32}$$
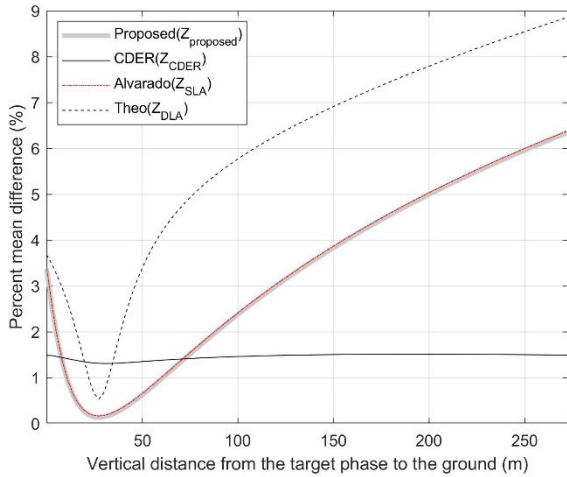
FIGURE 13. Average percent difference for different vertical distances.
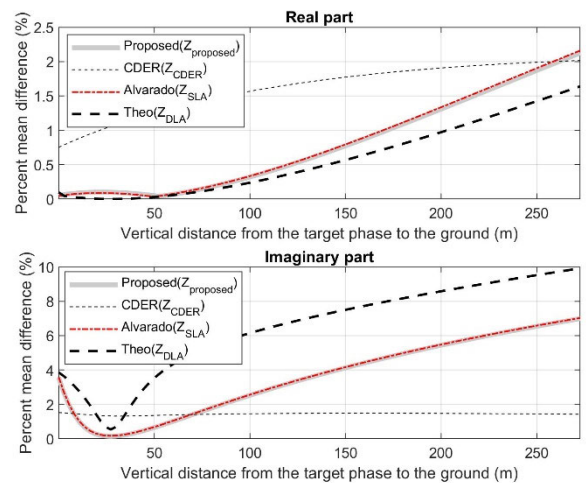

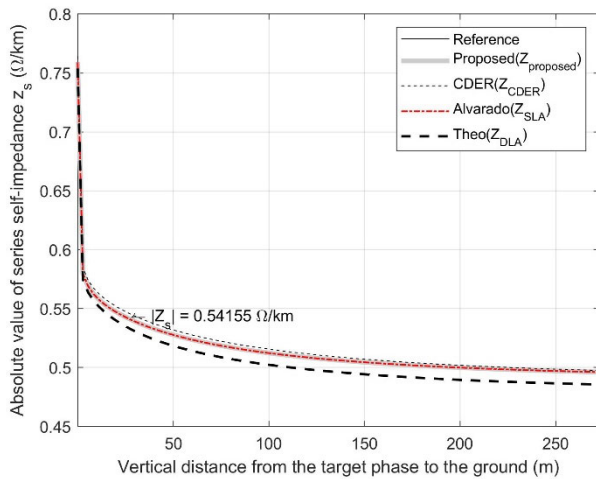**FIGURE 15.** Average percent differences for the real and imaginary parts.

FIGURE 14. Change in self-impedance (Z_{cc}) with the vertical distance of conductor bundle group *a*.

analytical model showed a higher difference than the proposed model, and therefore, it showed the largest difference in the absolute value of the self-impedance. For the imaginary part, before a distance of about 75 m, both the $\mathbf{Z}_{\mathrm{proposed}}$ and $\mathbf{Z}_{\mathrm{SLA}}$ models exhibited the least difference. By contrast, after about 75 m, the CDER model was more accurate than the proposed model. However, in the full range of the distance, the proposed method showed better accuracy than the compensated SLA model.

From Fig. 10 to Fig. 15, the $\mathbf{Z}_{\mathrm{proposed}}$ model slightly improved the $\mathbf{Z}_{\mathrm{SLA}}$ model. It is because both the models include the similar approximations derived in (8) and (18). To clarify the difference between both the models, Fig. 16 presents the average of the percent relative difference of both the models when the vertical and horizontal distances of the phase conductors in Fig. 9 change. In fact, the proposed model decreases the average of the percent relative difference. The proposed fourth term in (18) contribute the decrease in the relative difference. Thus, the proposed

method improves the previous model (e.g., Z_{SLA}). However, the difference between both the models for practical overhead lines with line sags, imbalances in phase conductors, and uncertainties of the frequency, ground resistivity, conductor characteristics (e.g., geometric mean radius and dc resistance), and transmission line structures (e.g., a single, double, or more circuit structure, and geometric mean distance), may be different from this case study. Therefore, the difference for the practical overhead lines will be examined in the second paper of this study.

B. CALCULATION SPEED COMPARISON
This study is to enhance the previous SLA in [14] by adding the fourth compensation term, which may create a heavy computational burden. Thus, this study measures calculation times of each method at a laptop computer (HP ZBook, Intel i7-7700HQ CPU @ 2.80GHz, 16.0 GB memory, and MATLAB 2019b). TABLE 4 presents the average calculation time in msec of each method on the frequency varying at $[f_{\mathrm{min}}, f_{\mathrm{max}}] = [0.1\ \mathrm{Hz}, 100\ \mathrm{kHz}]$. The total number of the calculations is 200. The simplified model ($\mathbf{Z}_{\mathrm{sim}}$) indicates the fastest speed because the second and HOTs of the IS are ignored for the self-impedance and the third and HOTs are neglected for the mutual impedance. In TABLE 2, the proposed method reduces the average percent difference to 0.02858% from 0.03229% (for $\mathbf{Z}_{\mathrm{SLA}}$), which means the improvement in the accuracy by as much as 11.49%. However, in TABLE 4, the proposed method increases the calculation time to 16.69% (for the two-conductor example in Fig. 2), 16.13% (for the distribution line example in Fig. 5), and 14.20% (for the transmission line example in Fig. 9) compared to that for $\mathbf{Z}_{\mathrm{SLA}}$. One of the applications of the proposed method is to evaluate the expected value of the self- and mutual impedances of overhead lines. Determining such an expected value via stochastic simulations requires a very large total number of calculations with fewer errors. After the tradeoff between improving the accuracy (e.g., 11.49%) and
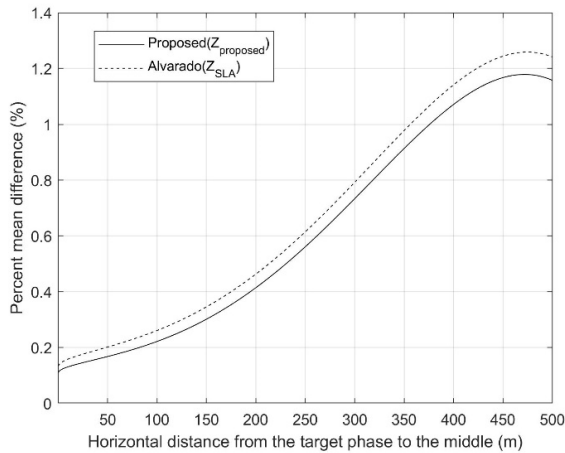
(a) Average of the percent relative difference when changing the horizontal distance
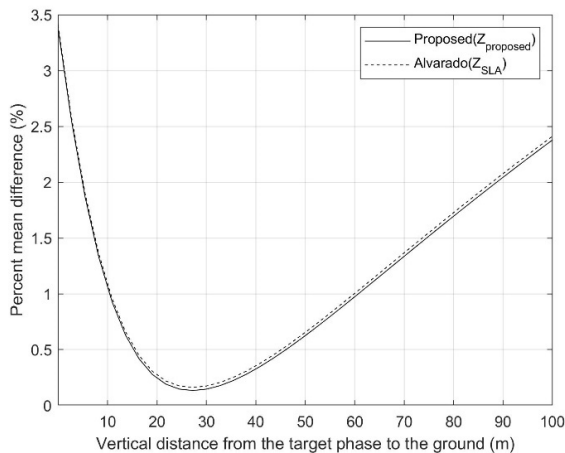
(b) Average of the percent relative difference when changing the vertical distance

FIGURE 16. Comparison of the proposed and Z_{SLA} models.

TABLE 4. Average calculation time (millisecond).

	$\mathbf{Z}_{sim}$	$\mathbf{Z}_{CDER}$	$\mathbf{Z}_{Theo}$	$\mathbf{Z}_{SLA}$	Proposed	% increase to $\mathbf{Z}_{SLA}$
Two conductors	0.20	0.23	0.95	0.86	1.00	16.69%
Distribution line	1.02	1.07	2.48	3.68	4.28	16.13%
Transmission line	8.19	8.43	18.69	27.28	31.15	14.20%

worsening the speed (e.g., 14.20%, 16.13%, or 16.69 %) is investigated, the proposed method that improves the accuracy will be adapted to the stochastic simulations, which will be presented in the second paper of this study.

V. CONCLUSION

A solution of the improper integral in COEs is required for estimating the series self- and mutual impedances of transmission and distribution lines. Therefore, many studies have approximated the improper integral (e.g., by using an SLA or a DLA model). However, the accuracy of the approximations can be improved. Thus, this study improves a previously proposed compensated SLA model by adding a fourth

compensation term. In the three case studies, the average percent differences of the previous models relative to the reference model were larger than those of the proposed model. In particular, the proposed model showed better accuracy than the compensated SLA model. For a distribution line example, simplified, analytical, CDER, and compensated SLA models show the average percent difference of 2.47008%, 3.95257%, 0.46305%, and 0.03229%. But the proposed method reduces the average percent difference to 0.029%, which means the improvement in the accuracy by as much as 11.49%. That is, this study presents a closed-form solution with smaller errors.

REFERENCES

[1] J. R. Carson, "Wave propagation in overhead wires with ground return," *Bell Syst. Tech. J.*, vol. 5, no. 4, pp. 539–554, Oct. 1926.
[2] F. Pollaczek, "On the field produced by an infinitely long wire carrying alternating current," *Elekztrische Nachrichten Technik*, vol. 3, 1926.
[3] U.-C. F. Alejandro, "Numerical infinite series solution of the ground-return Pollaczek integral," *Ingeniería, Investigación Tecnología*, vol. 16, pp. 49–58, 2015.
[4] A. C. S. Lima and C. Portela, "Closed-form expressions for ground return impedances of overhead lines and underground cables," *Int. J. Electr. Power Energy Syst.*, vol. 38, no. 1, pp. 20–26, Jun. 2012.
[5] Z. Li, J. He, B. Zhang, and Z. Yu, "Influence of frequency characteristics of soil parameters on ground-return transmission line parameters," *Electr. Power Syst. Res.*, vol. 139, pp. 127–132, Oct. 2016.
[6] A. C. S. Lima, R. A. R. Moura, M. A. O. Schroeder, and M. T. C. de Barros, "Assessment of different formulations for the ground return parameters in modeling overhead lines," *Electr. Power Syst. Res.*, vol. 164, pp. 20–30, Nov. 2018.
[7] M. Štumpf, "Evaluating the ground impedance—A new methodology based on EM reciprocity," *IEEE Trans. Electromagn. Compat.*, vol. 61, no. 3, pp. 928–934, Jun. 2019.
[8] J. Calvillo, F. A. Uribe, J. R. Morales, and R. Bernardino, "Implementation of conductor sub-division method for estimating ground-impedances," *IEEE Latin Amer. Trans.*, vol. 18, no. 6, pp. 1057–1065, Jun. 2020.
[9] F. A. Uribe, P. Zuniga, and E. Barocio, "Ground-impedance graphic analysis through relative error images," *IEEE Trans. Power Del.*, vol. 28, no. 2, pp. 1235–1237, Apr. 2013.
[10] I. Kim, "An approximate model for calculating three-phase line series impedance using the knee point selection method," *Int. Trans. Electr. Energy Syst.*, vol. 31, no. 4, 2021, Art. no. e12808.
[11] F. Tossani, F. Napolitano, F. Rachidi, and C. A. Nucci, "An improved approach for the calculation of the transient ground resistance matrix of multiconductor lines," *IEEE Trans. Power Del.*, vol. 31, no. 3, pp. 1142–1149, Jun. 2016.
[12] F. Tossani, F. Napolitano, and A. Borghetti, "Inverse Laplace transform of the ground impedance matrix of overhead lines," *IEEE Trans. Electromagn. Compat.*, vol. 60, no. 6, pp. 2033–2036, Dec. 2018.
[13] O. Ramos-Leaños, J. L. Naredo, F. A. Uribe, and J. L. Guardado, "Accurate and approximate evaluation of power-line earth impedances through the carson integral," *IEEE Trans. Electromagn. Compat.*, vol. 59, no. 5, pp. 1465–1473, Oct. 2017.
[14] F. L. Alvarado and R. Betancourt, "An accurate closed-form approximation for ground return impedance calculations," *Proc. IEEE*, vol. 71, no. 2, pp. 279–280, Feb. 1983.
[15] Á. Déri and G. Tevan, "Mathematical verification of Dubanton's simplified calculation of overhead transmission line parameters and its physical interpretation," *Archiv Elektrotechnik*, vol. 63, nos. 4–5, pp. 191–198, Jul. 1981.
[16] C. Dubanton, "Calcul approché des paramètres primaires et secondaires d'une ligne de transport, valeurs homopolaires (approximate calculation of primary and secondary transmission line parameters, zero sequence values)," *EDF Bull. Direction Études Reserches*, vol. 1, pp. 53–62, 1969.
[17] T. Noda, "A double logarithmic approximation of Carson's ground-return impedance," *IEEE Trans. Power Del.*, vol. 21, no. 1, pp. 472–479, Jan. 2006.
[18] I. Krolo, S. Vujević, and T. Modrić, "Highly accurate computation of carson formulas based on exponential approximation," *Electr. Power Syst. Res.*, vol. 162, pp. 134–141, Sep. 2018.

[19] P. C. Magnusson, V. K. Tripathi, G. C. Alexander, and A. Weisshaar, *Transmission Lines and Wave Propagation*. Boca Raton, FL, USA: CRC Press, 2000.

[20] C. Gary, "Approche complète de la propagation multifilaire en haute fréquence par utilisation des matrices complexes," *EDF Bull. Direction Études Recherches, Série B-Réseaux Électriques Matériels Électriques*, vols. 3–4, p. 5, 1976.

[21] J. R. Wait and K. P. Spies, "On the image representation of the quasi-static fields of a line current source above the ground," *Can. J. Phys.*, vol. 47, no. 23, pp. 2731–2733, Dec. 1969.

[22] E. D. Sunde, *Earth Conduction Effects in Transmission Systems*. New York, NY, USA: D. Van Nostrand Company, 1949.

[23] M. Pizarro and R. Eriksson, "Modeling of the ground mode of transmission lines in time domain simulations," in *Proc. 7th Int. Symp. High Voltage Eng.*, Dresden, Germany, 1991, pp. 179–182.

[24] T. Theodoulidis, "On the closed-form expression of Carson's integral," *Periodica Polytechnica Electr. Eng. Comput. Sci.*, vol. 59, pp. 26–29, 2015.

[25] A. Deri, G. Tevan, A. Semlyen, and A. Castanheira, "The complex ground return plane a simplified model for homogeneous and multi-layer earth return," *IEEE Trans. Power App. Syst.*, vol. PAS-100, no. 8, pp. 3686–3693, Aug. 1981.

[26] H. W. Dommel, *Electromagnetic Transients Program (EMTP) Theory Book*. Vancouver, BC, Canada: Microtran Power System Analysis Corporation, 1996.

[27] W. H. Kersting and R. K. Green, "The application of Carson's equation to the steady-state analysis of distribution feeders," in *Proc. IEEE/PES Power Syst. Conf. Expo.*, Phoenix, AZ, USA, Mar. 2011, pp. 1–6.

[28] W. H. Kersting, *Distribution System Modeling and Analysis*. Boca Raton, FL, USA: CRC Press, 2002.

[29] A. R. Bergen and V. Vittal, *Power Systems Analysis*, 2nd ed. Upper Saddle River, NJ, USA: Prentice-Hall, 2000.

[30] S. Butterworth, *Electrical Characteristics of Overhead Lines*. Leatherhead, U.K.: Electrical Research Association, 1954.

[31] E. Acha and M. Madrigal, *Power Systems Harmonics: Computer Modelling and Analysis*. Hoboken, NJ, USA: Wiley, 2001.

INSU KIM (Member, IEEE) received the Ph.D. degree from the Georgia Institute of Technology, Atlanta, in 2014. He is currently an Associate Professor in electrical engineering at Inha University, South Korea. His research interests include: analyzing the impact of stochastically distributed renewable energy resources such as photovoltaic systems, wind farms, and microturbines on distribution networks; examining the steady-state and transient behavior of distribution networks under active and reactive power injection by distributed generation systems; and improving power-flow, short-circuit, and harmonic analysis algorithms.

• • •